A New Model for Prediction of Drug Distribution in Tumor and Normal Tissues: Pharmacokinetics of Temozolomide in Glioma Patients

Lula Rosso,[1] Cathryn S. Brock,[1,2] James M. Gallo,[4] Azeem Saleem,[1,3] Patricia M. Price,[1,3] Federico E. Turkheimer,[1] and Eric O. Aboagye[1]

[1]Clinical Sciences Centre, Imperial College, Faculty of Medicine, Hammersmith Hospital Campus; [2]Imperial College Healthcare NHS Trust, London, United Kingdom; [3]Academic Department of Radiation Oncology, Christie Hospital NHS Trust, Manchester, United Kingdom; and [4]Department of Pharmaceutical Sciences, School of Pharmacy, Temple University, Philadelphia, Pennsylvania

Abstract

Difficulties in direct measurement of drug concentrations in human tissues have hampered the understanding of drug accumulation in tumors and normal tissues. We propose a new system analysis modeling approach to characterize drug distribution in tissues based on human positron emission tomography (PET) data. The PET system analysis method was applied to temozolomide, an important alkylating agent used in the treatment of brain tumors, as part of standard temozolomide treatment regimens in patients. The system analysis technique, embodied in the convolution integral, generated an impulse response function that, when convolved with temozolomide plasma concentration input functions, yielded predicted normal brain and brain tumor temozolomide concentration profiles for different temozolomide dosing regimens (75–200 mg/m^2/d). Predicted peak concentrations of temozolomide ranged from 2.9 to 6.7 μg/mL in human glioma tumors and from 1.8 to 3.7 μg/mL in normal brain, with the total drug exposure, as indicated by the tissue/plasma area under the curve ratio, being about 1.3 in tumor compared with 0.9 in normal brain. The higher temozolomide exposures in brain tumor relative to normal brain were attributed to breakdown of the blood-brain barrier and possibly secondary to increased intratumoral angiogenesis. Overall, the method is considered a robust tool to analyze and predict tissue drug concentrations to help select the most rational dosing schedules. [Cancer Res 2009;69(1):120–7]

Introduction

The development of new anticancer drugs still poses a considerable challenge. Of the many challenges, ensuring that optimal exposures of drug are achieved in tumor versus normal tissues is one of the most important (reviewed in refs. 1–3). The field of pharmacokinetics, which is concerned with the absorption, distribution, metabolism, and excretion of drugs, is instrumental to the drug development process and is applied to both preclinical and clinical investigations. The bulk of pharmacokinetic investigations assesses macropharmacokinetic characteristics such as drug clearance and oral bioavailability, key attributes that affect the successful development of a new drug entity. There has also been interest to apply pharmacokinetic models to characterize drug disposition in target tissues, such as tumors, the site of pharmacologic activity (reviewed in ref. 3). These efforts can reveal important mechanisms of drug distribution and also serve as a basis to predict the pharmacokinetic behavior of drugs in humans, particularly in tissues in which actual measurements cannot be readily obtained. In this regard, physiologically based and hybrid pharmacokinetic models that use rodent-to-human scale-up procedures have been used in an attempt to overcome the limitation of direct measurement of drug concentrations in tissues (4, 5). Although the effect of physicochemical properties and plasma protein binding on tissue drug distribution can be predicted fairly readily, these predictive pharmacokinetic models can be limited by uncertainties in the physiologic state and integrity of cell membranes, such as the blood-brain barrier, which can influence drug disposition, particularly in tumors that are known to be heterogeneous. To circumvent the issues related to the scale-up of preclinical models, we have used a positron emission tomography (PET) method to examine the tissue distribution of temozolomide directly in patients in conjunction with a convolution data analysis procedure. Temozolomide is an orally administered cytotoxic drug that has shown antitumor activity in glioma and melanoma (6–9), and in the United Kingdom, it has been approved as the standard of care for second-line therapy of patients with relapsed high-grade glioma and is licensed for use concurrently with radiotherapy for the primary treatment of glioblastoma multiforme. Although the systemic pharmacokinetics of this drug is known (10–12), little is known about its accumulation in tumors and normal tissues.

The direct noninvasive measurement of tissue drug concentrations afforded by our PET study in brain tumor patients suggested the use of a system analysis or convolution approach to generate a pharmacokinetic model. The essential features of the method require the definition of two functions: a unit impulse response function (IRF) and an input function describing the plasma drug concentration. The IRF expresses the drug concentration response of a given tissue region as though the drug is immediately delivered in the tissue of interest, analogous to a single instantaneous bolus injection (13). Under the conditions of system linearity, the IRF can be used to predict the response (i.e., tissue drug concentrations) for any plasma input function. The method can also similarly be applied to analyze and predict drug exposures in healthy tissue and, together with target tissue predictions, serve as an aid to design optimal dosing protocols. We believe that the assessment of drug disposition in target and normal tissue is sorely deficient in existing drug development

Requests for reprints: Eric O. Aboagye, Molecular Therapy and PET Oncology Research Group, Imperial College London, Faculty of Medicine, Hammersmith Hospital, Room 240 MRC Cyclotron Building, Du Cane Road, London W12 ONN, United Kingdom. Phone: 44-208-383-3759; Fax: 44-208-383-1783; E-mail: eric.aboagye@imperial.ac.uk.

doi:10.1158/0008-5472.CAN-08-2356

paradigms, and through the combined use of PET radiotracer studies and pharmacokinetic modeling, we show how these limitations can be addressed.

Materials and Methods

PET studies. Approval for the study was obtained from the Hammersmith Hospitals Research and Ethics Committee and the Administration of Radioactive Substances Advisory Committee of the United Kingdom. All patients gave written informed consent. The PET study was carried out in parallel with a phase I/II study of temozolomide [75–200 mg/m^2/d over 5 d every 28 d (phase II) or continuously over 6 to 7 wk (phase I)] for which the patient eligibility criteria have previously been described (10, 14). Patients had two scans: the first, before commencing treatment with oral temozolomide and the second during the first cycle of drug treatment. For the development of this method, we chose to study uniquely the second set of scans as we wanted to image the distribution of temozolomide in the presence of circulating "cold" doses of temozolomide. We analyzed a total of seven PET scans from patients with recurrent glioma, after oral temozolomide treatment with a phase II temozolomide regimen for five patients and phase I temozolomide regimen for two patients. For these patients, the [*methyl*-^{11}C]temozolomide PET studies were done on the last day of the phase I/II cycle at a median of 6 h (range, 1–16 h) after oral dosing. PET scans were done after injection of [*methyl*-^{11}C]temozolomide (average dose, 281 MBq; range, 165–356 MBq). The average amount of stable temozolomide injected was 1.1 μg (range, 0.5–1.6 μg) with an average specific activity of 53 GBq/μmol (range, 35–66 GBq/μmol). The original data were part of a doctoral thesis work by Dr. Cathryn Brock. [*methyl*-^{11}C] Temozolomide was prepared as previously described (15). Scanning was carried out at the Hammersmith Hospital using an ECAT 953 CTI Neuro-PET scanner (CTI/Siemens). An initial transmission scan was done using ^{68}Ge/Ga before tracer injection to correct for tissue attenuation. The radiolabeled temozolomide was given as an i.v. bolus over 30 s, starting 30 s after the start of scanning. PET data were collected in 21 time frames over 90 min (1 × 30 s, 1 × 15 s, 1 × 5 s, 1 × 10 s, 1 × 30 s, 4 × 60 s, 7 × 5 min, 5 × 10 min) with acquisition in the three-dimensional mode. The PET data were corrected for attenuation and detector efficiency and reconstructed into tomographic images using filtered back projection for the three-dimensional images of the brain studies (16). PET image data were then calibrated to megabecquerels per milliliter. All frames for each patient were summed to provide a high-quality image. Regions of interest were defined on 6 to 13 slices of whole tumor and contralateral brain with the aid of a recent computed tomography or magnetic resonance imaging film for each patient. Continuous online monitoring of peripheral arterial blood radioactivity was carried out throughout the scans (17). At discrete time points during the 90-min PET scans, blood samples were taken from patients; an aliquot was rapidly centrifuged to obtain corresponding plasma; and radioactivity concentration was measured in a NaI(TI) well counter for blood and plasma separately. The continuous blood counts were corrected using the plasma/blood ratio to derive a plasma input function. The plasma was further analyzed for radiolabeled metabolites using high-performance liquid chromatography. The plasma input function was corrected for the small quantity of [^{11}C]CO_2 and other unidentified radiolabeled metabolites that were detected in plasma during the scan.

System analysis. The pharmacokinetics of [*methyl*-^{11}C]temozolomide was evaluated using a linear system analysis approach (spectral analysis) that has been applied to PET data (13). Linear system analysis has been used for various pharmacokinetic applications, such as depicting drug absorption, and is viewed as an alternative to and more general than classic compartmental modeling (see review in ref. 18). In this regard, system analysis does not discern a compartmental structure for drug disposition as in classic compartmental modeling but rather relies on the convolution integral, which has the general form as follows;

$$C_{\text{out}}(t) = \int_0^t f_{\text{in}}(t-\tau)C_\delta(\tau)\mathrm{d}\tau \qquad \text{(A)}$$

where $C_{\text{out}}(t)$ is output function, $f_{\text{in}}(t)$ is input function, and $C_\delta(t)$ is impulse response function (IRF).

In the context of applying the convolution integral to temozolomide tissue concentration-time profiles, $C_{\text{out}}(t)$ would equal the temozolomide brain or brain tumor concentration-time profile; $f_{\text{in}}(t)$ would equal the input plasma concentration-time profile of temozolomide; and the impulse response function (IRF), $C_\delta(t)$, would represent the tissue disposition of temozolomide had the dose been delivered instantaneously to the tissue. The convolution approach as implemented here assumes time invariance and superposition. Time invariance means the response or output function is the same irrespective of when the input is initiated, whereas superposition indicates that for any constant multiple of the input [i.e., $A \cdot f_{\text{in}}(t)$], a corresponding multiple of the output is produced [i.e., $A \cdot C_{\text{out}}(t)$]. Knowledge of any two of the functions allows the third function to be determined by performing either convolution or deconvolution, and as such is a flexible approach to data analysis. The nature of the functions is dictated by the shape of the curve describing actual data, and thus, when the system involves drug disposition in plasma and tissues, exponential functions are often appropriate to describe the three functions associated with the convolution integral (Eq. A).

The exact form of the convolution integral used to analyze the temozolomide data can be resolved analytically as the sum of exponential functions as follows:

$$C_{\text{T}}(t) = \int_0^t \sum_{j=1}^{N} C_{\text{a}}(t-\tau)\cdot\alpha_j \exp(-\beta_j t)\mathrm{d}\tau \;\; \alpha_j \geq 0, \lambda \leq \beta_j \leq 1 \qquad \text{(B)}$$

where C_{T} and C_{a} represent the output and input functions, analogous to Eq. A, describing the measured temozolomide concentrations in tissue and plasma, respectively. Consistent with the assumptions of linear system analysis as mentioned above, the kinetics of temozolomide does not involve any saturable processes. Further, specific to the measurement of radiolabeled drugs, it was assumed that there are no radiolabeled metabolites in the organ of interest that contribute to the signal. Spectral analysis as implemented in Eq. B is a computational method used in PET to estimate the parameters in Eq. B, where $C_{\text{T}}(t)$ is the radioactivity concentration measured in a tissue region and $C_{\text{a}}(t)$ is the radioactivity concentration in the arterial plasma input. In spectral analysis, a large set of N predetermined exponential functions, which are characterized by two sets of coefficients, $\{\beta_j\}_{j\ =\ 1,N}$ and $\{\alpha_j\}_{j\ =\ 1,N}$, are fit to the actual data. The predetermined β values are chosen to cover the entire range of expected kinetic behavior, from λ, the decay constant of the radioisotope, which represents the slowest possible clearance detectable, to the faster measurable dynamics (i.e., transient component through tissue vasculature; ref. 19). The solution of Eq. B was found iteratively by optimizing the set of α values using the nonnegative least square algorithm (20). The values of the spectral coefficients are used to define the decay-corrected tissue IRF:

$$\text{IRF}(t) = \sum_{j=1}^{N} \alpha_j \exp(-(\beta_j - \lambda)t) \qquad \text{(C)}$$

and associated pharmacokinetic parameters as follows:

$$K_1 = \text{IRF}(t=0) = \sum_{j=1}^{N} \alpha_j \qquad \text{(D)}$$

$$\text{VD} = \int_0^\infty \text{IRF}(t)\mathrm{d}t = \sum_{j=1}^{N} \frac{\alpha_j}{\beta_j - \lambda} \qquad \text{(E)}$$

$$\text{MRT} = \frac{\text{VD}}{K_1} \qquad \text{(F)}$$

where K_1 is the rate for transport from plasma to tissue, VD is the distribution volume, and MRT is the mean residence time of the tracer in the tissue.

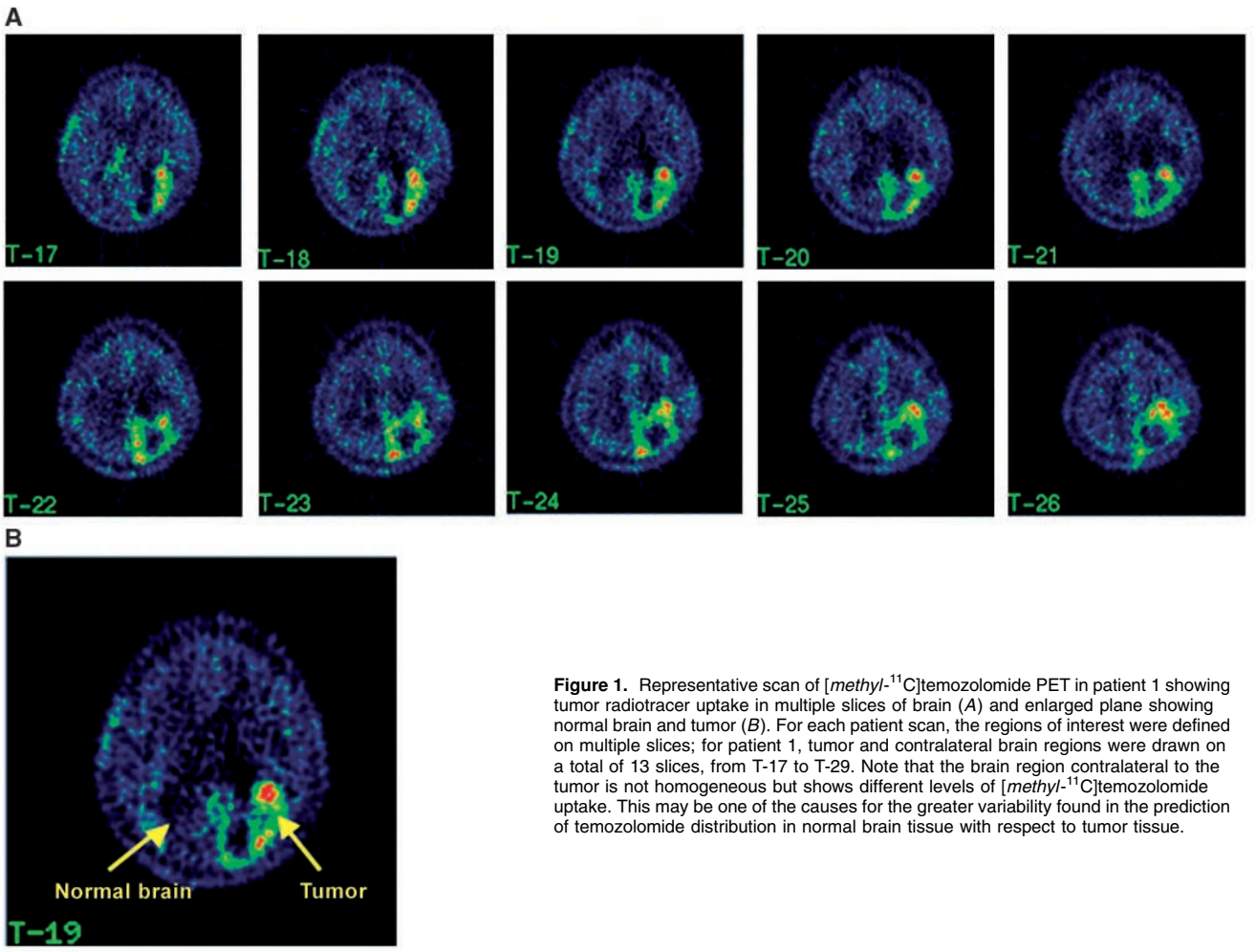

Figure 1. Representative scan of [*methyl*-^{11}C]temozolomide PET in patient 1 showing tumor radiotracer uptake in multiple slices of brain (*A*) and enlarged plane showing normal brain and tumor (*B*). For each patient scan, the regions of interest were defined on multiple slices; for patient 1, tumor and contralateral brain regions were drawn on a total of 13 slices, from T-17 to T-29. Note that the brain region contralateral to the tumor is not homogeneous but shows different levels of [*methyl*-^{11}C]temozolomide uptake. This may be one of the causes for the greater variability found in the prediction of temozolomide distribution in normal brain tissue with respect to tumor tissue.

It is then possible to predict the tissue response or output function, $C_T(t)$, by convolving the IRF with any given plasma input function, $C_a(t)$, via Eq. B. Note that if the IRF is determined using decaying inputs, as is often the case in PET studies, Eq. B needs to be decay corrected before being applied to nonradioactive plasma data.

Confidence intervals of spectral analysis parameters. Bootstrap analysis was done to provide an estimate of the error introduced by measurement and time extrapolation (21). This technique has been shown to require minimal assumptions about noise in the measurements, and in the absence of repeated measurements, it is the only consistent method for assessing uncertainty in all detected components of the tracer kinetic.

First, the residuals, ξ_k, are calculated as the difference between the estimated tissue concentration $C_T(t_k)$ and the measured tissue concentration $X(t_k)$ at each t_k time point:

$$\xi_k = (X(t_k) - C_T(t_k))\sqrt{w_k^2} \quad k = 1, 2, \ldots, M \qquad \text{(G)}$$

where M is the number of time points. In PET experiments, the measurement error varies with time. w_k is the weight at time k, proportional to the SD of the measurement at time k. The residuals, $\{\xi_k\}$, are therefore a finite sample of the error distribution. To simulate the effect of measurement noise on the spectral analysis estimates, we generated a new set of "measured" data by adding resampled residuals to the original estimate. For a more detailed discussion, see ref. 22. The residuals $\{\xi_k\}$ were then resampled randomly without substitution to form a new set of residuals ξ_k^* that were added to the estimated $C_T(t_k)$ values. The weights themselves were not resampled and were reassigned at the appropriate time point. In other words, the bootstrapped set of residuals were used to generate a "new" data set defined as

$$X^*(t_k) = C_T(t_k) + \frac{\xi_k^*}{\sqrt{w_k^2}} \quad k = 1, 2, \ldots, M \qquad \text{(H)}$$

Taking $X^*(t_k)$ as the new "measured" temozolomide tissue concentrations, the spectral analysis provided a new set of N α, $\{\alpha_j^*\}_{j = 1,\ldots, N}$, best fit coefficients, based on the nonnegative least square algorithm, which described the tissue disposition of temozolomide. The bootstrap procedure was repeated R times, generating R sets of the N amplitudes $\{\alpha_j^{*(i)}\}_{j = 1,\ldots, N}$, $i = 1,\ldots, R$, to obtain a statistically significant estimate of their distribution and R sets of estimated tissue concentrations $C_T(t_k)^{(i)}$, using Eq. B. Finally, the distributions of the bootstrapped $C_T(t_k)^{(i)}$ ($i = 1,\ldots, R$) for each scan were then used to calculate the respective 95% confidence intervals.

Predictions of tissue exposures based on nonradioactive plasma pharmacokinetic data. Because the PET studies were limited to 90 min, and we preferred to predict the disposition of temozolomide over longer time periods, we use three clinical temozolomide regimens and the associated published plasma temozolomide data to generate unique plasma input functions. This not only would facilitate a complete assessment of temozolomide exposure but also would provide a means to contrast tumor and normal tissue exposures of temozolomide under clinically relevant conditions. The first dosing regimen consisted of temozolomide given as a single oral dose of 100 mg/m^2/d daily for 5 consecutive days every 28 d (11); this will be referred to as protocol A. The second dosing regimen consisted

of temozolomide given as a single oral dose of 200 mg/m^2/d daily for 5 consecutive days every 28 d (11); this will be referred to as protocol B. The third regimen consisted of temozolomide given as continuous oral schedule of 75 mg/m^2/d daily for 7 wk (10); this will be referred to as protocol C.

The three unique plasma input functions were convolved with the IRF determined by PET spectral analysis. This procedure provides a time-dependent function, $C_T(t)$ (see Eq. B), of either temozolomide normal brain or brain tumor concentrations. Subsequently, from $C_T(t)$, the total tissue exposure to temozolomide was estimated as the area under the concentration-time curve (AUC). The tissue AUC was computed up to specified times, and not extrapolated to infinity, by trapezoidal numerical integration of the predicted tissue concentration-time curve using Matlab 7.1 (MathWorks Limited).

Results

PET analysis of temozolomide tumor and normal brain radiotracer distribution. Representative transverse slices of the cumulative [*methyl*-^{11}C]temozolomide uptake over 90 minutes are shown in Fig. 1. These types of figures served as the basis to select regions of interest that were manually traced around tumor and contralateral normal brain in several slices (ranging from 6 to 13, depending on size of tumor). Given the signal intensity averaged over the multislice regions of interest and the metabolite-corrected [*methyl*-^{11}C]temozolomide plasma input function, we used spectral analysis to solve Eq. B iteratively to yield a small set of non-zero α parameters, which defined the separate region of interest IRF for each patient. The group average spectra and group average IRF were derived by averaging all seven patients' scans.

Typically, the convolution analysis of Eq. B required just a few exponential terms, with three required in tumor and only two in normal brain. These results were consistent in all scans studied, as well as in previous [*methyl*-^{11}C]temozolomide PET quantification studies done without prior oral administration of temozolomide (23). As anticipated and consistent with a variable and compromised blood-brain barrier in brain tumors, radiotracer uptake was heterogeneous within tumors (Fig. 1). At the same time, normal brain regions showed greater than expected variations in radiotracer uptake.

The kinetic parameters associated with the disposition of [*methyl*-^{11}C]temozolomide that were derived from the IRFs are shown in Table 1. The transport rate, K_1, of temozolomide into brain tumor was greater than that into normal brain and is consistent with a more permeable blood-brain barrier in tumor. The cumulative exposure of temozolomide was also greater in brain tumor compared with normal brain (see VD values in Table 1); however, the mean residence time (MRT) was essentially equal in both tissue compartments and indicated that the efflux of temozolomide from brain tumor to plasma was also higher than in normal brain. The kinetic parameters calculated excluding the blood volume in the two tissue spaces yielded similar trends for both K_1 and VD (see Table 1). However, the MRT in normal brain was ~3-fold greater than in tumor, which may reflect the greater contribution of the normal brain blood volume, as opposed to the blood volume in tumor, to the overall tissue disposition of temozolomide. In essence, the characteristics of the blood-brain barrier, due to either breakdown or active angiogenesis, in brain tumor facilitate rapid and greater drug penetration, yet is coupled with a similarly rapid exit back into plasma, making the tissue residence time no greater than that achieved in normal brain.

The variability of the IRF as determined by spectral analysis was estimated by a bootstrapping procedure (21). We then used the ensemble of bootstrapped solutions to estimate the 95% confidence interval of the model predicted tissue levels obtained with the mean IRF. One advantage of the bootstrapping technique is it allows robust statistical estimates of characteristics of a system when actual data are limited. Given the rigor of performing PET investigations in brain tumor patients, repeated measurements in the same region will not be possible; thus, reliance on a bootstrap procedure is in order. A number of iterations (R = 1,000), based on the observed experimental error, were done in conjunction with the bootstrap procedure. Representative bootstrapped solutions for the normal brain and tumor IRF of patient 1 are shown in Fig. 2*A* and *B*. In addition, we calculated the 95% confidence interval of the bootstrapped IRF solutions averaged over all seven patients for both tumor and brain tissue and extrapolated them up to 24 hours (data not shown). The confidence intervals for the IRF in tumor and normal brain were comparable and higher at earlier times, as expected when temozolomide concentrations are changing rapidly. From ~3 hours, the 95% confidence intervals continued to decline to very small values and became negligible after 12 hours.

Prediction of temozolomide tissue distribution from nonradioactive plasma data. The nonradioactive plasma data were convolved with the group average human PET temozolomide IRF to calculate tissue concentrations of the drug under different clinically used dosing schedules. The short elimination half-life of temozolomide ensures that there is minimal drug accumulation

Table 1. Mean distribution volume and K_1 values of [*methyl*-^{11}C]temozolomide in human tissue

ROI	*n*	*m*	VD$^{(1)}$	VD$^{(2)}$	K_1 (s^{-1})	MRT (s)
Normal Brain	7	58	0.93 (0.46)	0.52 (0.08)	0.033 (0.016)	39 (31)
Tumor	7	58	1.41 (0.58)	0.92 (0.11)	0.052 (0.025)	38 (30)
Parameter values excluding contribution from blood volume						
Normal Brain	7	58	0.90 (0.46)		0.0003 (0.0001)	3,400 (1,600)
Tumor	7	58	1.35 (0.58)		0.0016 (0.0009)	1,000 (600)

NOTE: VD$^{(1)}$, K_1, and MRT (mean residence time) were calculated using spectral analysis (12) and averaging over m slices from scans of n patients; VD$^{(2)}$ was calculated using the rank-shaped estimator (28). Tissue pharmacokinetic parameters derived with and without contribution of regional blood volume are presented. The SDs are in parentheses.
Abbreviation: ROI, region of interest.

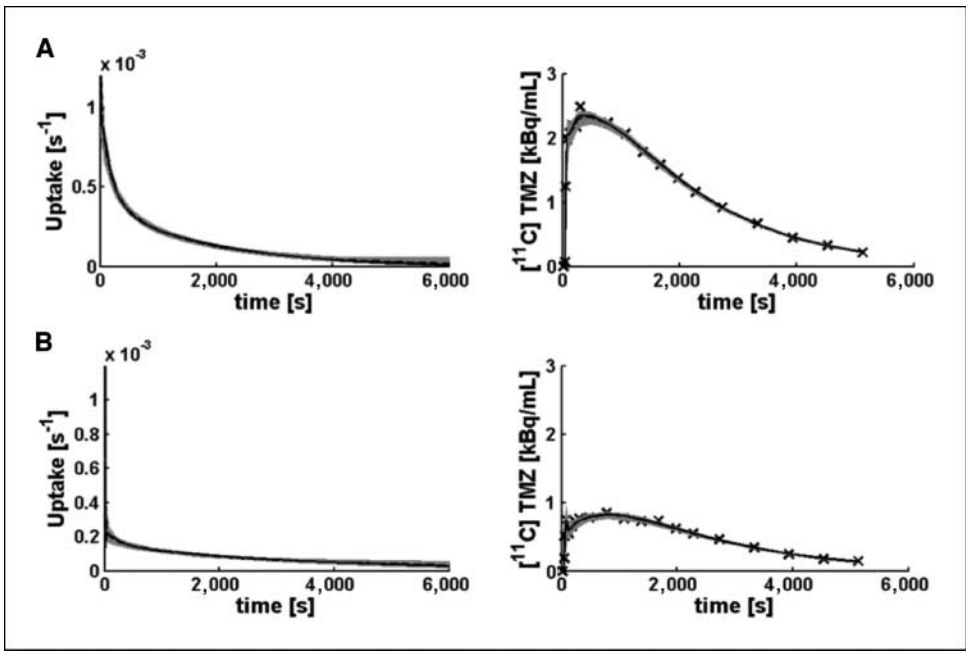

Figure 2. Representative bootstrap analysis for the PET scan from patient 1, with R = 1,000 iterations. *A,* tumor IRF (*left*) and tissue distribution (*right*). *B,* normal brain IRF (*left*) and tissue distribution (*right*). The curves shown are the bootstrapped unbiased solution (*black solid line*), original tissue data (*cross*), and all bootstrapped solutions (*gray*), to indicate PET scan measurement noise. As expected, the biggest variance occurs at the early time points. *TMZ,* temozolomide.

on successive doses for each of the three oral dosing regimens, and supports our assumption that saturable kinetics would not be found in tissues. We also implicitly assumed that the IRF derived from the PET studies is the same as the IRF at full dose (i.e., principle of superposition) in each of the clinical dosing schemes despite the more prolonged duration (90 minutes versus 24 hours) of the plasma input functions. The resulting predicted temozolomide concentration profiles in brain tumor and normal brain are shown in Fig. 3*A* and *B*, respectively, for each of the three clinical regimens. Regardless of the temozolomide treatment regimen, peak temozolomide brain tumor concentrations were greater than peak normal brain concentrations, and the predicted tumor and normal brain profiles became indistinguishable within error after 6 hours. The cumulative tissue exposures as measured by the AUC for the different dosing regimens are reported in Table 2. The AUC, calculated to 24 hours, in brain tumor was always greater than the corresponding normal brain AUC, and ranged from 18.91 to 40.37 μg/mL·h, compared with a range of 12.86 to 27.47 μg/mL·h in normal brain. For comparison, the plasma AUC (calculated up to 24 hours) for the different dosing regimens followed the same trend as the predicted tissue AUC: 13.96 μg/mL·h for protocol A, 30.56 μg/mL·h for protocol B, and 16.83 μg/mL·h for protocol C. Hence, temozolomide tissue-to-plasma exposure ratios over a 24-hour period were ~1.3 for glioma and ~0.9 for normal brain. Finally, brain and tumor tissue terminal half-life ($t_{1/2}$) values were very similar in all protocols, being 3.05 hours (protocol A), 3.17 hours (protocol B), and 3.08 hours (protocol C) in brain tumor, and 3.04 hours (protocol A), 3.15 hours (protocol B), and 3.07 hours (protocol C) in normal brain. The predicted normal brain temozolomide concentrations were more variable than those in brain tumor as evidenced by the 95% confidence intervals (Fig. 3*C* and *D*).

Discussion

Of the several investigational new anticancer drugs being developed, ~40% fail in early clinical development because of inappropriate pharmacokinetics (24). The decision to terminate drug development due to pharmacokinetic failures has often been attributed to either poor systemic properties of rapid drug elimination or poor oral bioavailability. With the advent of targeted drugs and an increasing realization that target tissue concentrations can determine the therapeutic efficacy of a drug, the ability to predict drug exposures in tissues of drug activity and toxicity can provide critical information on the prospects of successful drug development. It is established that the ability to make early decisions to terminate drug development on drugs that will ultimately fail will significantly reduce clinical costs (25–27). Similarly, by shifting 5% of all clinical failures from phase III/regulatory to the phase I setting could also reduce clinical costs by 5.5% to 7.1% (25). Thus, development of predictive pharmacokinetic models and incorporation of their results into an early-phase clinical drug development decision paradigm should produce significant savings. The pharmacokinetic approach offered in the current investigation provides a means to extract important information on drug disposition in tissues and to subsequently develop pharmacokinetic models that can predict drug disposition under conditions in which data have not been obtained.

The predictive method described in this article relies on administration of trace quantities of an isotopically radiolabeled positron-emitting drug during dosing (oral or parenteral) of the nonradioactive drug. Injection of the radiolabeled compound is followed by PET imaging to generate a mathematical description of the blood and tissue kinetics of the drug. The mathematical approach used here is governed by the doctrine of linear system analysis that relies on the convolution integral to relate input and output of the system. The method does not require defining the potentially complex compartmental structure for drug distribution but rather defines a unique IRF for the tissue using spectral analysis. Although PET data were analyzed individually, it was essential to estimate the mean and confidence interval for this patient population to enable the methods to be applied to individual patient plasma (cold temozolomide) data. The average IRF could then be convolved with any plasma profile from separate pharmacokinetic studies of the nonradioactive drug to determine

tissue distribution of the drug in that pharmacokinetic study, assuming linear kinetics. In the past, we have used spectral analysis to describe the pharmacokinetics of labeled anticancer drugs in the absence of a full dose of the drug (23). Here we describe a general modeling approach using a PET-IRF (generated in the presence of the full dose of nonlabeled drug) to predict tissue distribution kinetics from plasma pharmacokinetic data obtained in a non-imaging study.

The PET coupled linear system approach as applied here operates within the clinical domain to make predictions of drug disposition in tissues. A comparison can be made with predictions of human pharmacokinetic properties from sophisticated scaled preclinical models (4). The preclinical pharmacokinetic models are physiologically based and often cast as hybrid pharmacokinetic models. These models are sufficiently distinct from the linear system–based models and warrant further consideration. The physiologically based hybrid models represent the tissue of interest in terms of anatomic and physiologic attributes, and when combined with drug-specific characteristic of protein binding or membrane transport, are considered mechanistic-based models for drug disposition. Features of nonlinearity such as saturable membrane transport, tissue binding, or time-dependent effects can be accounted for in the hybrid techniques but not in the linear system approach. Animal-based hybrid models have been extrapolated to patients, yet, as with any predictive tool, require actual patient data for validation. Thus, the hybrid pharmacokinetic approach is viewed as a mechanistic-based approach initiated in a preclinical phase that can be scaled to humans, whereas the PET coupled-linear system analysis method is directly applicable to human pharmacokinetic data.

We have used the DNA alkylator temozolomide as the prototypical example of the PET-IRF method (6–9). Consistent with a previous study (23), the IRF derived from all the PET scans indicated that the main differences between tumor and contralateral normal brain were faster drug delivery to tumor in the first 30 minutes and a greater total exposure, possibly due to breakdown of the blood-brain barrier and increased neovascularization. However, Meikle and colleagues (23) reported a rather high tumor/normal brain VD ratio of 7.8, whereas we found a ratio of 1.5 (Table 1). Direct comparison may not be possible because the previous study was done in one patient who received tracer only doses of [*methyl*-^{11}C]temozolomide and was not undergoing active treatment with oral temozolomide as in this study. We further confirmed the VD obtained with a rank-shaped estimator, which has been shown to reduce the noise in VD estimation by optimizing the choice of the basis set (28). Temozolomide showed little tumor selectivity beyond 6 hours with concentration-time profiles quite similar in each tissue. This is in keeping with previous studies in which temozolomide was radiolabeled at different positions on the ring with carbon-11 to elucidate its mechanism of action; it was noted that ring-opening and triazine formation was not selective to tumor (17). The more rapid penetration of temozolomide in brain tumor early after drug administration was sufficient to lead to greater drug exposure in tumor compared to normal brain, with brain tumor/normal brain AUC ratio being 1.47 for each of three clinical dosing protocols. It is of some interest to compare the current study results to those predicted by a hybrid pharmacokinetic model of temozolomide in brain derived from rat studies (5), particularly because this model was validated in brain tumor patients using only available CSF temozolomide concentrations (29). The rat hybrid model and extrapolated human model for temozolomide in brain tissues were based on unbound temozolomide concentrations and not on total as used here. A conversion from unbound to total temozolomide concentrations can be approximated by using the ratios of the influx to efflux rate constants previously reported (5), and yields a total AUC for 24 hours in brain tumor of 48 μg/mL·h for protocol B, which is quite consistent with the predicted value of 40.37 μg/mL·h (see Table 2). Using the same conversion approach for the hybrid model–predicted normal brain temozolomide AUC yields a value of 123 μg/mL·h or ~4-fold greater than the value predicted by the PET-linear system approach. A simulation study was conducted in the study of Zhou and colleagues (5) to reflect the variability in the

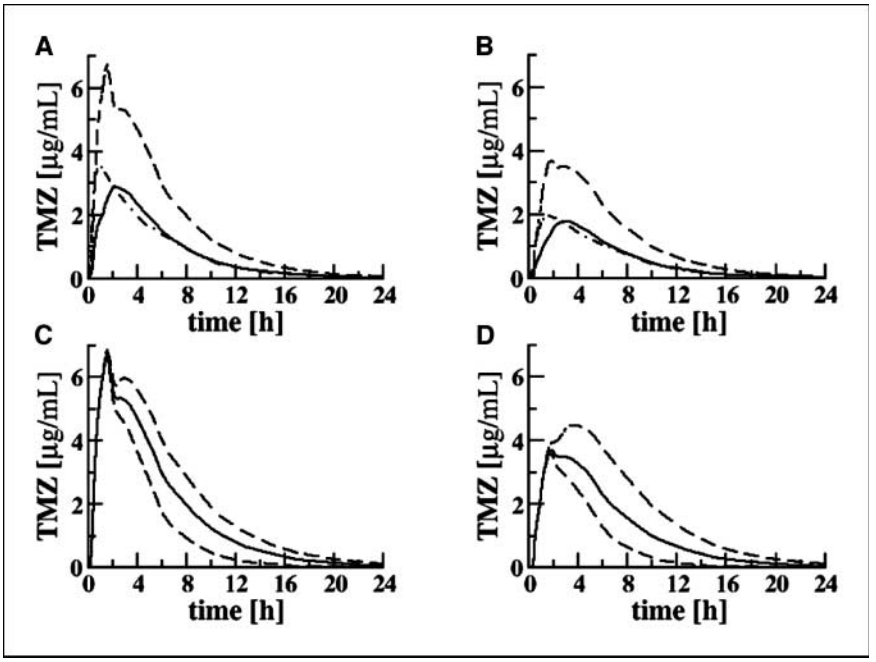

Figure 3. Predicted temozolomide tissue distribution for protocol A (*solid line*), protocol B (*dashed line*), and protocol C (*dot-dashed line*) in tumor (*A*) and normal brain (*B*). The prediction was based on use of the mean IRF generated from different tissue volumes of multislice dynamic PET scans in the different regions of interest, excluding the blood pool component in tissue. Representation of prediction variability in tumor (*C*) and normal brain (*D*) obtained with protocol B; the average predicted tissue drug levels (*solid line*) together with the predicted 95% confidence interval (*dashed line*) are shown. Protocol A: single oral dose of 100 mg/m^2/d daily for 5 consecutive days every 28 d. Protocol B: single oral dose of 200 mg/m^2/d daily for 5 consecutive days every 28 d. Protocol C: continuous oral schedule of 75 mg/m^2/d daily for 7 wk.

Table 2. Predicted temozolomide tissue AUC values for the considered dosing and schedule protocols

	$AUC_{6\ h}$ (μg/mL·h)	$AUC_{12\ h}$ (μg/mL·h)	$AUC_{24\ h}$ (μg/mL·h)
Protocol A			
Brain tumor	12.50	17.57	18.91
Normal brain	7.79	11.80	12.86
Protocol B			
Brain tumor	26.82	37.38	40.37
Normal brain	16.81	25.12	27.47
Protocol C			
Brain tumor	13.67	18.62	19.92
Normal brain	8.66	12.53	13.55

NOTE: Protocol A: single oral dose of 100 mg/m^2/d daily for 5 consecutive days every 28 d. Protocol B: single oral dose of 200 mg/m^2/d daily for 5 consecutive days every 28 d. Protocol C: continuous oral schedule of 75 mg/m^2/d daily for 7 wk.
The AUC values have been derived integrating the predicted tissue concentration-time curve from 0 to 6 h ($AUC_{6\ h}$), from 0 to 12 h ($AUC_{12\ h}$), and from 0 to 24 h ($AUC_{24\ h}$). The predicted tissue concentration was obtained by convolution analysis using the average human PET-derived IRF and the nonradioactive plasma temozolomide concentration in different dosing protocols, using Eq. B.

brain tumor AUC due to altered blood-brain barrier permeability and fractional tumor blood volume. These simulations revealed that the temozolomide brain tumor AUC could vary ~6-fold, which, if used to estimate the brain tumor to normal brain AUC ratio, would encompass the 1.47 value found here. Thus, it seems that both the hybrid model and linear system approaches are in general agreement, and which method one chooses may be based on available resources, modeling preferences, and stage of implementation in the drug development paradigm.

The PET-IRF predicted temozolomide brain tumor concentrations at a dose of 200 mg/m^2 (protocol B) were ≥2 μg/mL for 8 hours, ≥1 μg/mL for 12 hours, and ≥0.04 μg/mL within a 24-hour period. In preclinical studies, Raymond and colleagues (30) showed that continuous exposure to temozolomide at concentrations of 0.02, 0.2, and 2 μg/mL decreased clonogenic survival by ≥50% in 9%, 16%, and 35%, respectively, of 101 tumors taken directly from patients and grown *in vitro* in soft agar. The response rates achieved with temozolomide may thus be related, at least in part, to its pharmacokinetics.

Analysis of drug accumulation in normal tissues should indicate the likelihood of toxicity; however, most often there are no established drug concentration-toxicity relationships in organs of toxicity. This type of endeavor is a large undertaking even in a rodent model, and most often blood and its cellular components are used as surrogates to define pharmacokinetic-pharmacodynamic relationships in patients. In our study, we were able to measure temozolomide concentrations in normal brain, which currently do not serve as means to set dose-limiting toxicities, but rather provide a means to assess blood-brain barrier function. A whole-body PET scan would be required to determine drug accumulation in all major organs, and this type of analysis may be most warranted when preclinical studies indicate dose-dependent organ toxicity or low therapeutic indexes. In summary, we report the use of a flexible linear system analysis model for predicting tumor and normal tissue pharmacokinetics derived from human PET studies. The unique feature of the modeling technique is the IRF to describe drug disposition in tissue, which can be linked to any human plasma drug concentration-time profile under the condition of system linearity. The resultant tissue drug concentration profiles can characterize drug transport rates and accumulation that can be used as a tool to evaluate different dosing schemes in terms of drug efficacy and, possibly, drug toxicity. The PET-linear system approach could find general application in early-phase clinical drug development strategies to facilitate decisions about future therapeutic potential of new anticancer drugs.

Disclosure of Potential Conflicts of Interest

No potential conflicts of interest were disclosed.

Acknowledgments

Received 6/23/2008; revised 9/16/2008; accepted 10/16/2008.

Grant support: United Kingdom Medical Research Council, Cancer Research UK Grant C2536/A5708 (E.O. Aboagye), and NIH grant CA72937 (J.M. Gallo).

The costs of publication of this article were defrayed in part by the payment of page charges. This article must therefore be hereby marked *advertisement* in accordance with 18 U.S.C. Section 1734 solely to indicate this fact.

References

1. Gelmon KA, Eisenhauer EA, Harris AL, Ratain MJ, Workman P. Anticancer agents targeting signaling molecules and cancer cell environment: challenges for drug development? J Natl Cancer Inst 1999;91:1281–7.
2. Rousseau A, Marquet P. Application of pharmacokinetic modelling to the routine therapeutic drug monitoring of anticancer drugs. Fundam Clin Pharmacol 2002;16:253–62.
3. Workman P, Aboagye EO, Chung YL, et al. Minimally invasive pharmacokinetic and pharmacodynamic technologies in hypothesis-testing clinical trials of innovative therapies. J Natl Cancer Inst 2006; 98:580–98.
4. Gallo JM, Vicini P, Orlansky A, et al. Pharmacokinetic model-predicted anticancer drug concentrations in human tumors. Clin Cancer Res 2004;10:8048–58.
5. Zhou QY, Guo P, Kruh GD, Vicini PL, Wang XM, Gallo JM. Predicting human tumor drug concentrations from a preclinical pharmacokinetic model of temozolomide brain disposition. Clin Cancer Res 2007;13:4271–79.
6. Mutter N, Stupp R. Temozolomide: a milestone in neuro-oncology and beyond? Expert Rev Anticancer Ther 2006;6:1187–204.
7. Oreilly SM, Newlands ES, Glaser MG, et al. Temozolomide—a new oral cytotoxic chemotherapeutic agent with promising activity against primary brain-tumors. Eur J Cancer 1993;29A:940–42.
8. Payne MJ, Pratap SE, Middleton MR. Temozolomide in the treatment of solid tumours: current results and rationale for dosing/scheduling. Crit Rev Oncol Hematol 2005;53:241–52.
9. Danson SJ, Middleton MR. Temozolomide: a novel oral alkylating agent. Expert Rev Anticancer Ther 2001; 1:13–9.
10. Brock CS, Newlands ES, Wedge SR, et al. Phase I trial of temozolomide using an extended continuous oral schedule. Cancer Res 1998;58:4363–7.
11. Hammond LA, Eckardt JR, Baker SD, et al. Phase I and pharmacokinetic study of temozolomide on a daily-for-5-days schedule in patients with advanced solid malignancies. J Clin Oncol 1999;17:2604–13.
12. Rudek MA, Donehower RC, Statkevich P, Batra VK, Cutler DL, Baker SD. Temozolomide in patients with advanced cancer: phase I and pharmacokinetic study. Pharmacotherapy 2004;24:16–25.
13. Cunningham VJ, Jones T. Spectral analysis of dynamic PET studies. J Cereb Blood Flow Metab 1993; 13:15–23.
14. Brock CS, Young H, O'Reilly SM, et al. Early evaluation of tumour metabolic response using [F-18]fluorodeoxyglucose and positron emission tomography: a pilot study following the phase II chemotherapy

schedule for temozolomide in recurrent high-grade gliomas. Br J Cancer 2000;82:608–15.
15. Brown GD, Luthra SK, Brock CS, Stevens MFG, Price PM, Brady F. Antitumor imidazotetrazines. 40. Radiosyntheses of [4-C-11-carbonyl]- and [3-*N*-C-11-methyl]-8-carbamoyl-3-methylimidazo[5,1-*d*]-1,2,3,5-tetrazin-4(3*H*)-one (temozolomide) for positron emission tomography (PET) studies. J Med Chem 2002;45:5448–57.
16. Kinahan PE, Rogers JG. Analytical 3D image reconstruction using all detected events. IEEE Trans Nucl Sci 1989;36:964–68.
17. Saleem A, Brown GD, Brady F, et al. Metabolic activation of temozolomide measured *in vivo* using positron emission tomography. Cancer Res 2003;63:2409–15.
18. Zhou H. Pharmacokinetic strategies in deciphering atypical drug absorption profiles. J Clin Pharmacol 2003;43:211–27.
19. Turkheimer F, Moresco RM, Lucignani G, Sokoloff L, Fazio F, Schmidt K. The use of spectral analysis to determine regional cerebral glucose utilization with positron emission tomography and [F-18]fluorodeoxyglucose—theory, implementation, and optimization procedures. J Cereb Blood Flow Metab 1994;14:406–22.
20. Lawson CL, Hanson RJ. Solving least square problems. Englewood Cliffs (NJ): Prentice Hall; 1974.
21. Turkheimer F, Sokoloff L, Bertoldo A, et al. Estimation of component and parameter distributions in spectral analysis. J Cereb Blood Flow Metab 1998;18:1211–22.
22. Efron B, Tibshirani R. An introduction to the bootstrap. New York: Chapman & Hall; 1993.
23. Meikle SR, Matthews JC, Brock CS, et al. Pharmacokinetic assessment of novel anti-cancer drugs using spectral analysis and positron emission tomography: a feasibility study. Cancer Chemother Pharmacol 1998;42:183–93.
24. Wang J, Urban L. The impact of early ADME profiling on drug discovery and development. Drug Discov World 2004;5:73–86.
25. DiMasi JA. The value of improving the productivity of the drug development process: faster times and better decisions. Pharmacoeconomics 2002;20 Suppl 3:1–10.
26. DiMasi JA, Caglarcan E, Wood-Armany M. Emerging role of pharmacoeconomics in the research and development decision-making process. Pharmacoeconomics 2001;19:753–66.
27. DiMasi JA, Grabowski HG. Economics of new oncology drug development. J Clin Oncol 2007;25:209–16.
28. Turkheimer FE, Hinz R, Gunn RN, Aston JAD, Gunn SR, Cunningham VJ. Rank-shaping regularization of exponential spectral analysis for application to functional parametric mapping. Phys Med Biol 2003;48:3819–41.
29. Ostermann S, Csajka C, Buclin T, et al. Plasma and cerebrospinal fluid population pharmacokinetics of temozolomide in malignant glioma patients. Clin Cancer Res 2004;10:3728–36.
30. Raymond E, Izbicka E, Soda H, Gerson SL, Dugan M, Von Hoff DD. Activity of temozolomide against human tumor colony-forming units. Clin Cancer Res 1997;3:1769–74.

A New Model for Prediction of Drug Distribution in Tumor and Normal Tissues: Pharmacokinetics of Temozolomide in Glioma Patients

Lula Rosso, Cathryn S. Brock, James M. Gallo, et al.

Cancer Res 2009;69:120-127.